Sulphur Poisoning, Water Vapour and Nitrogen Dilution Effects on Copper-based Catalyst Dynamics, Stability and Deactivation during CO_2 Reduction Reactions to Methanol

Supporting information

*Anže Prašnikar, Blaž Likozar**

Department of Catalysis and Chemical Reaction Engineering, National Institute of Chemistry, Hajdrihova 19, 1001 Ljubljana, Slovenia

1 Peclet number calculation

The molecular diffusion of all species involved was calculated using equation by Fuller, Schettler and Giddings [S1]:

$$D_{AB} = \frac{10^{-2} T^{1.75} \left(\frac{1}{M_A} + \frac{1}{M_B}\right)^{1/2}}{p_{tot}[(\sum_A v_i)^{1/3} + (\sum_B v_i)^{1/3}]^2} \left[\frac{m^2}{s}\right]. \quad \text{(S1)}$$

The MeOH diffusion coefficient for typical composition (inlet ratio H_2/CO_2=3, x(MeOH, H_2O and CO)=4%,4% and 1% respectively was calculated using equation by Fairbanks and Wilke[S2].

$$D_{m,i} = \frac{1}{\sum_{j=1, j\neq i}^{N} \frac{y_j}{D_{ij}}}, \quad \text{(S2)}$$

The temperature dependence of viscosity was determined using equation (equation S3) of Sutherland[S3]. Since H_2, CO_2 and N_2 make up the majority of gas phase, we took only those into account. The coefficients of below correlation can be found in Table S1.

$$\eta = \lambda \frac{T^{3/2}}{T + C} \quad \text{(S3)}$$

Table S1. Coefficients for the calculation of viscosity

Gas	C (K)	λ (Pas $K^{-0.5}$)
H_2	72	0.6362 10^{-6}
CO_2	240	1.572 10^{-6}

N_2	111	$1.407\ 10^{-6}$

The gas mixture viscosity was determined using mixing rule[S4]:

$$\eta = \frac{\sum y_i \eta_i (M_i)^{0.5}}{\sum y_i (M_i)^{0.5}} \quad \text{(S4)}$$

The axial Peclet number (Pe_{ax}) was calculated using equation given by Guedes de Carvalho and Delgado [5,6]. The results are displayed in the table below:

Table S2. The parameters for calculation of axial Peclet number.

T [°C]	P [bar]	H_2/CO_2 inlet ratio	GHSV [1/h]	V(cat-volume) [mL]	Bed porosity [/]	d(reactor-diameter) [mm]	d(particle-diameter) [mm]	L(bed-length) [cm]	**Peclet (axial bed H_2O) [/]**	Peclet (axial bed MeOH) [/]
240	50	3	6000	1	0.4	6.35	0.3	3.2	**86**	126
240	20	3	6000	1	0.4	6.35	0.3	3.2	**87**	128
360	20	3	6000	1	0.4	6.35	0.3	3.2	**75**	113
360	50	3	6000	1	0.4	6.35	0.3	3.2	**75**	111

In the case of H_2O the rate of convective flow is minimally 75 times higher than the rate of diffusion mass transport meaning than plug flow reactor model can describe process with sufficient accuracy.

2 Reaction products-induced deactivation modelling

Equation 1 from the main text in differential form:

$$\int_0^a da(p,t) = \int_0^t a(p,t)^n \left(A_{H2O} e^{-\frac{Ea_{H2O}}{RT(t)}} p_{H2O}^m(p,t) + k_{thermal}(T) \right) dt \quad \text{(S5)}$$

In difference form:

$$a(p,t) = a(p,t-\Delta t(t)) + a(p,t)^n \left(A_{H2O} e^{-\frac{Ea_{H2O}}{RT(t)}} p_{H2O}^m(p,t) + k_{thermal}(T) \right) \Delta t(t) \quad \text{(S6)}$$

Here Δt(t) represents the time intervals between GC sampling. Validation by integrating activity part of the equation, while the time derivative was integrated numerically:

Differential form:

$$a(p,t) = \left(1 - (1-n)A_{H2O}\int_{o}^{t} e^{-\frac{Ea_{H2O}}{RT(t)}} p_{H2O}^{m}(t)dt\right)^{\frac{1}{1-n}} \quad (S7)$$

Numerical form:

$$a(p,t) = \left(1 - (1-n)A_{H2O}\sum_{i=0}^{n(t)} e^{-\frac{Ea_{H2O}}{RT(t)}} p_{H2O}^{m}(t)\Delta t(t)\right)^{\frac{1}{1-n}} \quad (S8)$$

In figure below, we can observe that we practically obtain the same results.

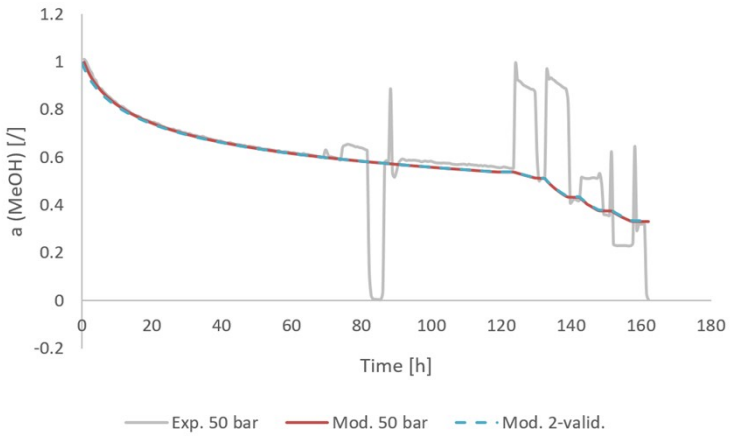

Figure S1. Validation of the model using model equation n. 2 (Eq. S8) using data of CuCeAl test at 50 bar.

Below is a chart of the average ageing composition determination and the estimated error with other methods.

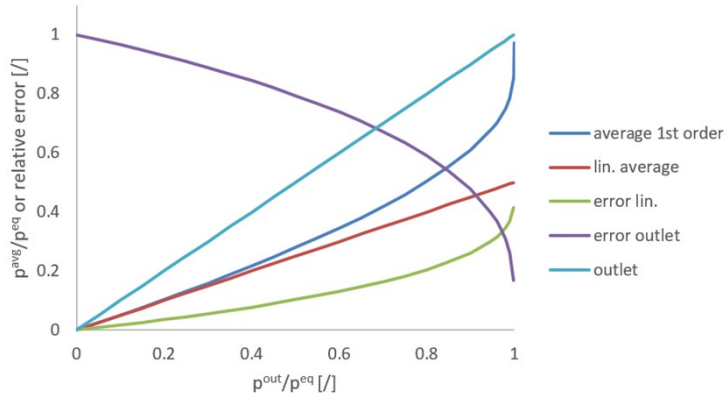

Figure S2. Dark blue line: The average ageing composition in the dependance of p^{out}/p^{eq}. Red line: Linear average is calculated using inlet and outlet partial pressures. Light blue line: Outlet composition. Green and violet lines are errors estimation based on average 1st order line.

3 Rietveld refinement

The list of phases can be find in the Table S3.

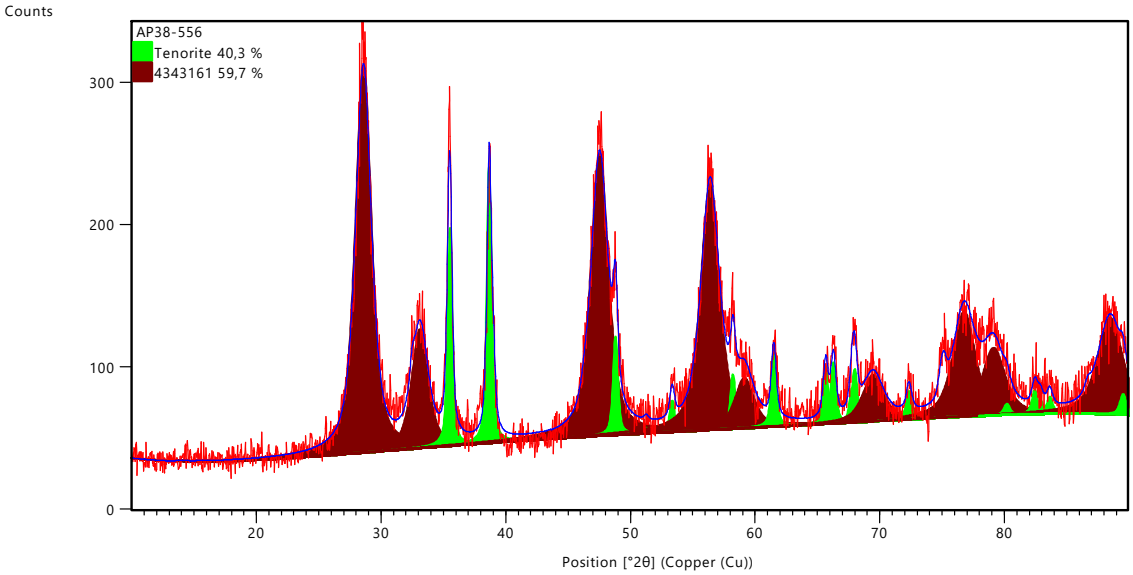

Figure S3. Rietveld refinement of XRD diffractogram of CuCeAl sample. Software colours the area starting from low to high angles. In this process smaller peaks can be overshadowed by larger peaks at higher angles. Example is covering of peak at 75° which corresponds to Cu(-222). The fitted line from Rietveld analysis describes the experimental data with sufficient accuracy.

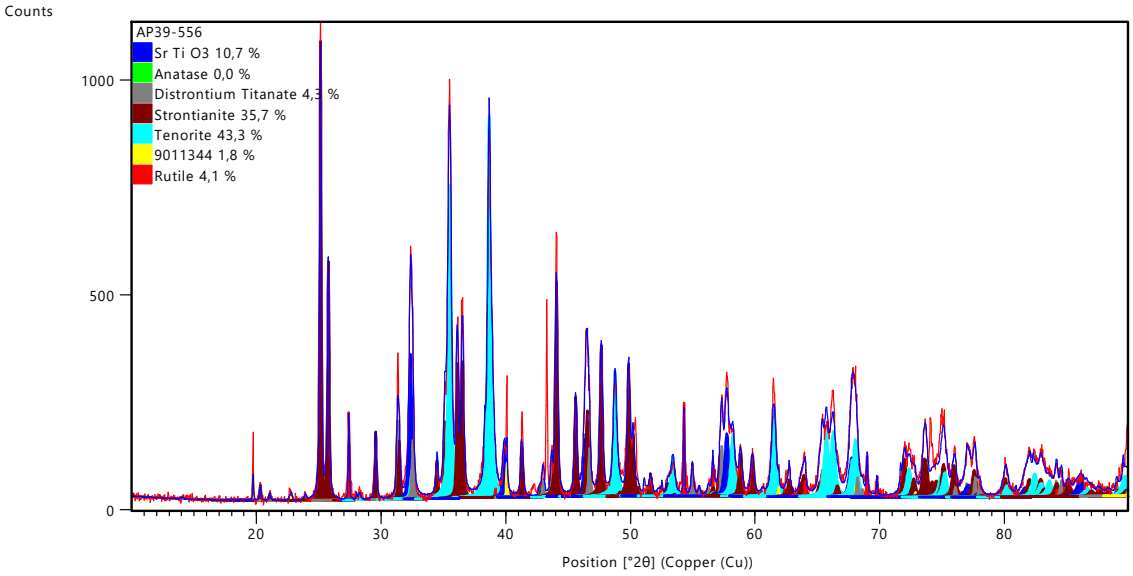

Figure S4. Rietveld refinement of XRD diffractogram of CuSrTi sample.

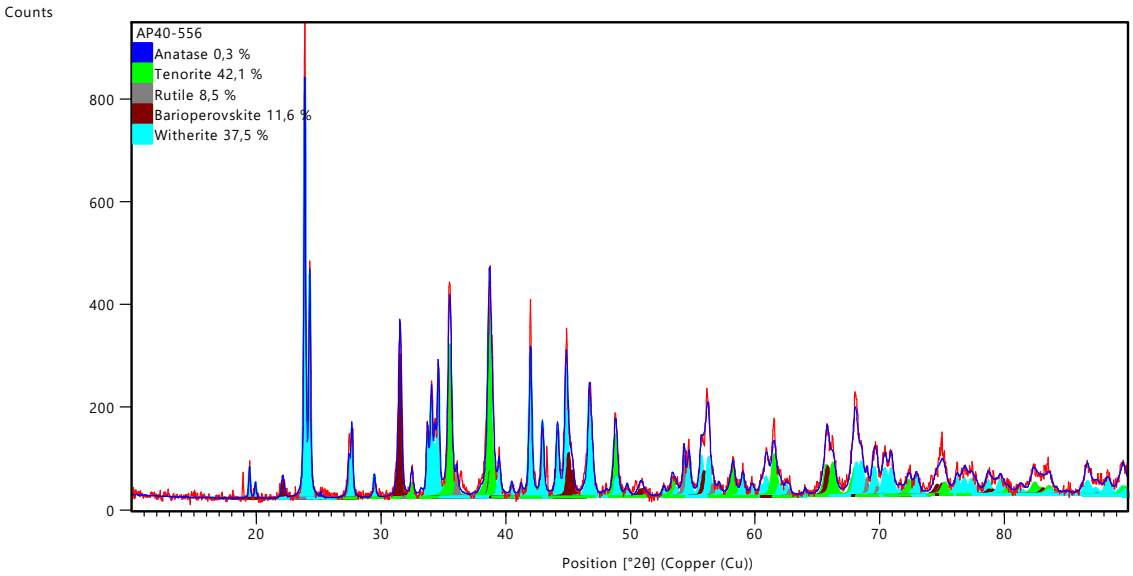

Figure S5. Rietveld refinement of XRD diffractogram of CuBaTi sample.

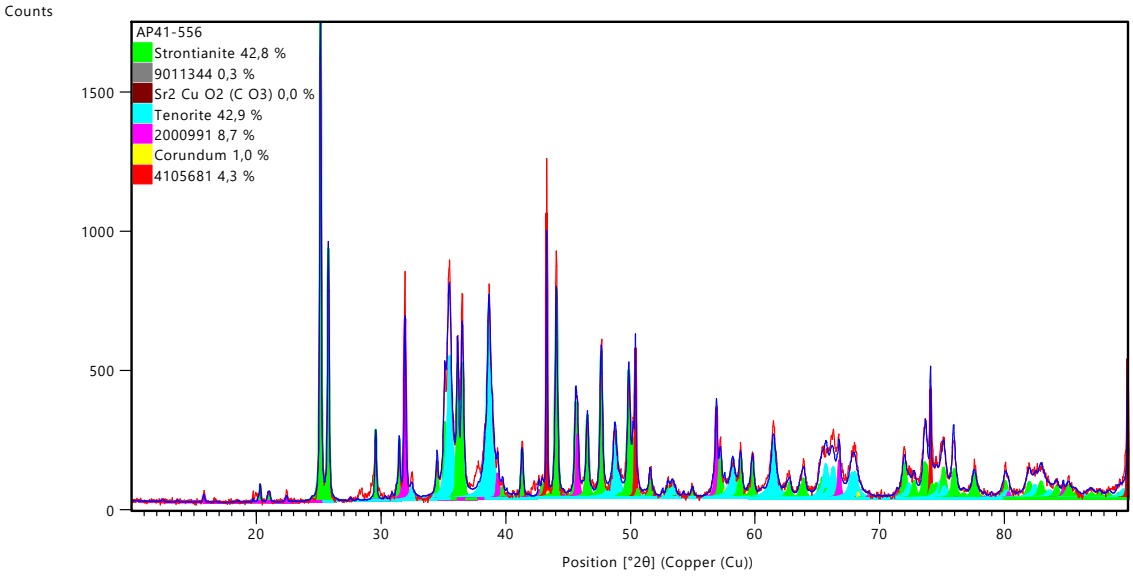

Figure S6. Rietveld refinement of XRD diffractogram of CuSrAl sample.

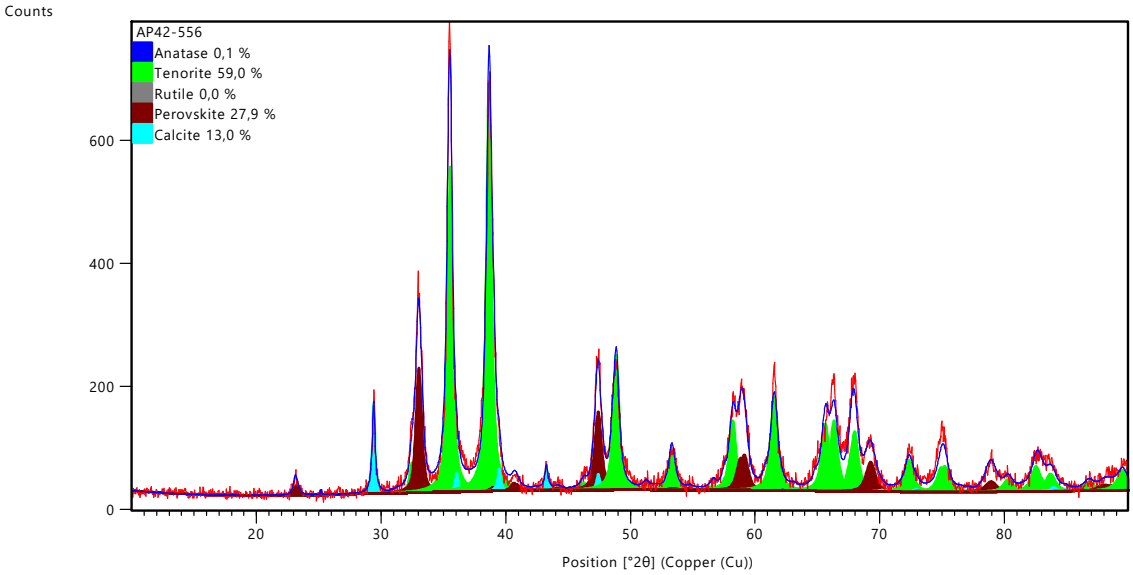

Figure S7. Rietveld refinement of XRD diffractogram of CuCaTi sample.

Table S3. List of PANalytical X'Pert HighScore Plus references.

Name	Material	Reference code (PANalytical X'Pert HighScore Plus)
4343161	CeO_2	96-434-3162
Tenorite	CuO	96-901-5925
Sr Ti O3	$SrTiO_3$	96-231-0688
Strontianite	$SrCO_3$	96-901-3803
Rutile	TiO_2	96-900-9084
Anatase	TiO_2	96-900-8217
Distrontium Titanate	Sr_2TiO_4	96-151-7789
9011344	$Sr(NO_3)_2$	96-901-1345
Barioperovskite	$BaTiO_3$	96-901-4775
Witherite	$BaCO_3$	96-901-3806
2000991	$SrAl_2O_4$	96-200-0992
Corundum	Al_2O_3	96-900-9680
Perovskite	$CaTiO_3$	96-900-2802
Calcite	$CaCO_3$	96-901-6707
4105681	Cu	96-410-5682

The Rietveld refinement of CuZnAl after reduction can be found in our previous work.[7]

4 Effect of nitrogen on methanol synthesis

For determination of nitrogen effect on methanol synthesis we used three different catalysts: CuBaTi, CuCeAl and CuSrTi with three different characteristics. Catalysts CuBaTi and CuSrTi have different strengths of basic sites, while catalyst CuCeAl also contains CeO_x redox sites. However they all contain copper, which is used in all industrial low-pressure methanol synthesis catalysts. In this way, nitrogen effect could be comprehensively assessed.

Effect of nitrogen concentration in feed gas on concentration of methanol and carbon monoxide was studied under following conditions:

- Pressure: 20 bar
- Temperature: 240 °C
- Constant molar flow rate
- Feed comp.: $^{H_2/CO_2} = 3$

Nitrogen concentration was varied between 0, 10 and 30 volume %. Raw data of reactor effluent concentration is shown in Table S4. Effect is shown on Figure S8 for catalyst CuBaTi. Nitrogen concentration was first increased from 0 to 30 vol. % and then decreased gradually back to 0 vol. % by 10 vol. % intervals. Carbon monoxide and methanol concentration in reactor outlet gas followed opposite trend to nitrogen. Both concentrations decreased as nitrogen concentration increased and increased back to almost original value as nitrogen concentration was reduced back to 0 vol. %. Since

carbon monoxide and methanol concentrations after nitrogen addition experiments (Number of experiment 5) are approximately the same as prior to nitrogen addition (Number of experiment 1) it can be concluded that nitrogen presence does not cause irreversible catalyst deactivation. This can be expected because nitrogen molecules are very stable and high pressures and temperatures with presence of appropriate iron catalyst are needed to activate it for combination with hydrogen (Haber-Bosch process). Reaction rates were then normalized to sum of hydrogen and carbon dioxide partial pressures.

Table S4. Molar fractions of CO, CO_2, H_2, H_2O and CH_3OH at reactor effluent at 240 °C, 20 bar a and inlet molar ratio of H_2 to CO_2 of 3 at different concentration of nitrogen.

N_2 concentration [vol. %]	CO [vol. %]	CO_2 [vol. %]	H_2 [vol. %]	H_2O [vol. %]	CH_3OH [vol. %]
0.8	0.3	24.4	74.0	0.8	0.4
31.4	0.2	15.2	53.4	0.6	0.2
21.5	0.2	17.9	60.2	0.6	0.3
11.2	0.3	21.0	67.1	0.7	0.3
0.8	0.3	24.4	73.9	0.8	0.4

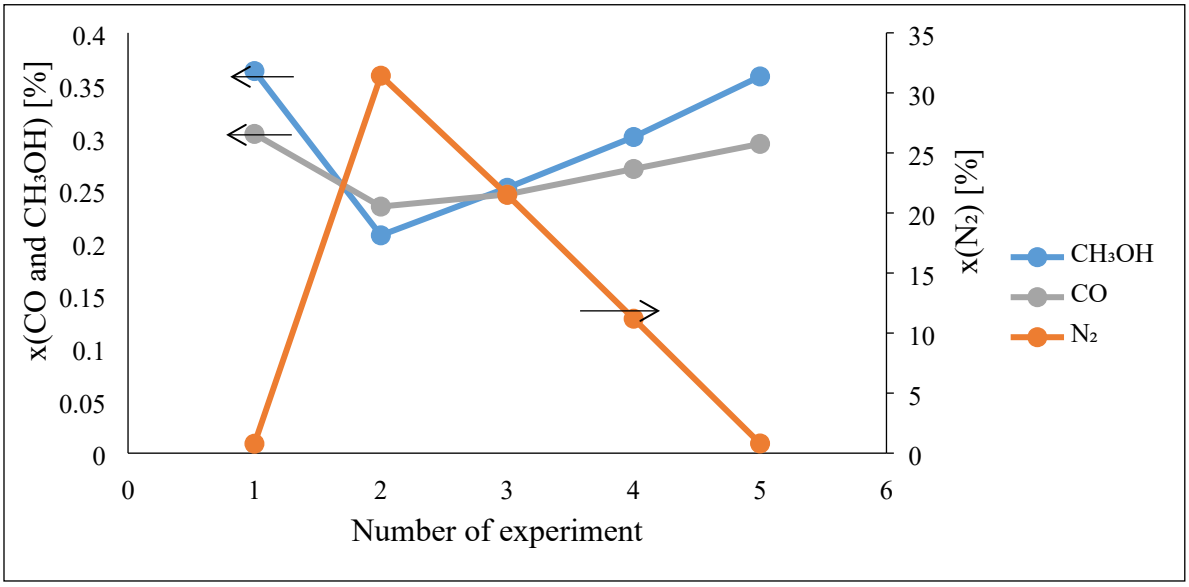

Figure S8. Effect of nitrogen content on carbon monoxide and methanol outlet molar fraction for CuBaTi.

Results of normalization are shown on Figure S9 and Figure S10 for methanol and carbon monoxide formation respectively. On average 14 % decrease of methanol production rate and a 10 % increase of carbon monoxide production rate can be observed at nitrogen concentration of 30 vol. %. Trend holds for all three catalyst types studied. Difference between normalized production rates for different could be more attributed to experimental error than to actual difference in catalytic performance. Effect of nitrogen on normalized reaction rates can be explained by effect of chemical equilibrium.Table S5 gives results of equilibrium calculation with Aspen Plus V9 software. Gibbs type reactor with *Calculate phase equilibrium and chemical equilibrium* calculation option selected was used for calculations. Effluent molar flow rates correspond to chemical equilibrium condition. Equilibrium conversion of reactants (X_{eq}) from data in is calculated as:

$$X_{eq} = \frac{\dot{F}_{H_2,f} + \dot{F}_{CO_2,f} - \left(\dot{F}_{H_2,e} + \dot{F}_{CO_2,e}\right)}{\dot{F}_{H_2,f} + \dot{F}_{CO_2,f}} = \frac{3\frac{kmol}{h} + 1\frac{kmol}{h} - \left(2.68\frac{kmol}{h} + 0.82\frac{kmol}{h}\right)}{3\frac{kmol}{h} + 1\frac{kmol}{h}} = 0.125 \quad \text{(S9)}$$

where $\dot{F}_{H_2,f}$ is molar flow rate of hydrogen at reactor inlet, $\dot{F}_{CO_2,f}$ molar flow of carbon dioxide at reactor inlet and $\dot{F}_{H_2,e}$, $\dot{F}_{CO_2,e}$ molar flow rates of hydrogen and carbon dioxide at reactor outlet.

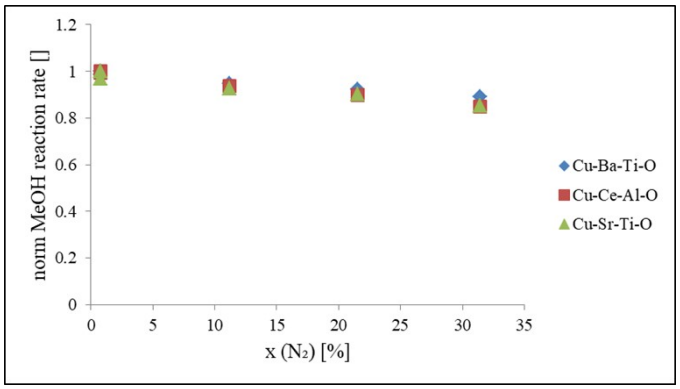

Figure S9. Normalized methanol production rate dependence on nitrogen concentration for CuBaTi, CuCeAl and CuSrTi catalyst.

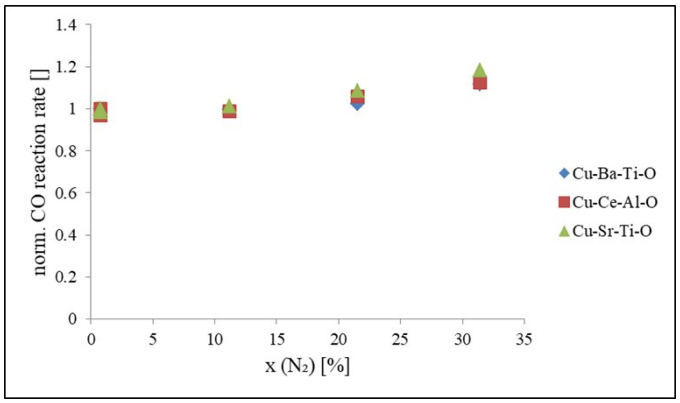

Figure S10. Normalized carbon monoxide production rate dependence on nitrogen concentration for CuBaTi, CuCeAl and CuSrTi catalysts.

Table S5. Equilibrium reactor simulation in Aspen Plus V9 for methanol synthesis reactions.

Parameter	Unit	Feed	Effluent
Temperature	°C	240	240
Pressure	bar a	20	20
Molar flow rate of CO	kmol/h	0	0.11
Molar flow rate of CO_2	kmol/h	1	0.82
Molar flow rate of CH_3OH	kmol/h	0	0.07
Molar flow rate of H_2	kmol/h	3	2.68

Molar flow rate of N_2	kmol/h	0	0
Molar flow rate of H_2O	kmol/h	0	0.18

Table S6 gives results of equilibrium conversion, obtained with Aspen Plus V9 simulation as above and conversion calculate by above equation for all four levels of nitrogen concentration studied experimentally. Reaction conditions are 240 °C and 20 bar a.

Table S6. Dependency of equilibrium conversion of reactants on nitrogen concentration at 240 °C temperature and 20 bar a pressure.

Nitrogen concentration [vol.%]	Equilibrium conversion of hydrogen and carbon dioxide [%]
0	12.5
10	11.9
20	9.3
30	9.0

It can be clearly seen, that equilibrium conversion falls with increasing nitrogen concentration. Ratio of actual to equilibrium conversions can now be calculated. Actual conversion for stoichiometric composition at reactor inlet and small change of volume due to reaction progress is calculated as:

$$X = \frac{y_{CO} + y_{CH_3OH}}{\left(1 - y_{N_2}\right)} \qquad \text{(S10)}$$

where X is conversion (of carbon dioxide), y_{CO}, y_{CH3OH} and y_{N2} are molar fractions of carbon monoxide, methanol and nitrogen. Results are shown in Table S7. Conversions of carbon dioxide ranged from 13.9 % and 15.2 % of equilibrium conversion. Figure S11 shows that with increasing sum of pressure of reactants (carbon dioxide and hydrogen), the equilibrium molar fraction of CO decreases, while CH_3OH molar fraction raises. Trend of formation rates closely follows trend of equilibrium composition of both methanol and carbon monoxide. Total pressure of reactants, of course, is smaller at given overall total pressure partial pressure of nitrogen is higher.

Table S7. Ratios between measured CO_2 conversion and equilibrium CO_2 conversion.

x(N_2) [%]	Conversion(CO_2)/conversion(CO_2)-eq [%]
0.0	14.2
31.4	15.2
21.5	14.5
11.2	14.1
0.0	13.9

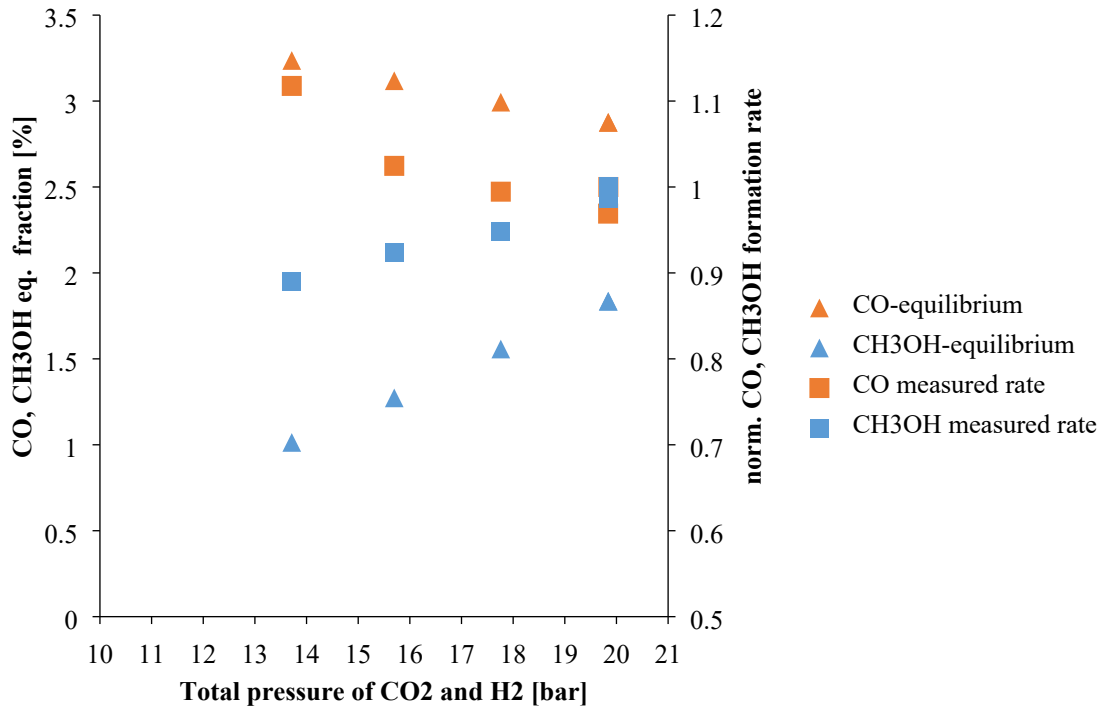

Figure S11. Dependency of equilibrium fractions of carbon monoxide and methanol and formation rate of carbon monoxide and methanol on total pressure of carbon dioxide and hydrogen.

This leads to the explanation that nitrogen only acts as a diluting agent and that the partial pressures of hydrogen and carbon dioxide are important variables for determining methanol and carbon monoxide formation kinetics.

5 Calculation of MeOH productivity

The equation also include the flow correction due to decrease the number of mols for MeOH synthesis.

$$MeOH\ \text{Productivity} = \frac{GHSV \cdot (1 - 2x_{MeOH}^{out})}{22.4\ \text{L/mol}} \cdot x_{MeOH}^{out} \cdot M_{MeOH} \quad \text{(S11)}$$

6 References

1 E. N. Fuller, P. D. Schettler and J. C. Giddings, *Ind. Eng. Chem.*, 1966, **16**, 551.

2 D. F. Fairbanks and C. R. Wilke, *Ind. Eng. Chem.*, 1950, **42**, 471–475.

3 W. Sutherland, *Philos. Mag. Ser. 5*, 1893, **36**, 507–531.

4 A. Pohar, D. Belavič, G. Dolanc and S. Hočevar, *J. Power Sources*, 2014, **256**, 80–87.

5 J. R. F. Guedes de Carvalho and J. M. P. Q. Delgado, *AIChE J.*, 2003, **49**, 1980–1985.

6 J. M. P. Q. Delgado, *Heat Mass Transf.*, 2006, **42**, 279–310.

7 A. Prašnikar, A. Pavlišič, F. Ruiz-Zepeda, J. Kovač and B. Likozar, *Ind. Eng. Chem. Res.*, 2019, **58**, 13021–13029.